Time-division multiplexed resistive pulse sensor on a microfluidic chip

Gihoon Choi, Erica Murphy, and Weihua Guan*
Department of Electrical Engineering, Pennsylvania State University, University Park, USA
*w.guan@psu.edu

***Abstract*— Due to its simplicity and robustness, resistive pulse sensors have been widely used to detect, measure, and analyze particles at length scales ranging from nanometers to micrometers. While multiple pore-based resistive pulse sensors are preferred to increase the analysis throughput and to overcome the clogging issues, the scalability is often limited. Here we reported a microfluidic time-division multiplexing accessing (TDMA) single-end resistive pulse sensor, in which particles can be analyzed through a scalable number of microfluidic channels. This multiplexed approach is effective in measuring the particle size and concentration, in analyzing the particle arriving dynamics, and in discriminating mixed populations. It also provides a robust mechanism to overcome the clogging issue, allowing the analysis to continue even when some of the pores are clogged.**

Keywords*— *resistive pulse sensor, micropore, nanopore, time-division multiple access, microfluidics

I. INTRODUCTION

Resistive pulse sensor [1-30] would require measuring sufficient numbers of single particle translocations to generate meaningful statistics for analysis. In this regard, multichannel systems have a clear advantage in terms of faster data collection and analysis throughput. Integration of multiple channels into the same device also enables the analysis of the same sample with different experimental parameters such as applied voltage and pore size. Besides, multiple pores also help to keep the analysis running even one or few of the pores are clogged, a grand challenge in resistive pulse sensors[31, 32]. In recognition of these benefits, efforts to multiplex the recording was pursued in micropores[33] and nanopores[34-36]. However, the device scalability is limited because each fluidic channel requires a separate measuring apparatus. An ideal multiplexed resistive pulse sensor should have a single output to interface with the data acquisition hardware easily.

In this work, we reported a microfluidic time-division multiplexing accessing (TDMA) single-end resistive pulse sensor for particle analysis. In the cellular communication field, TDMA allows multiple users to communicate with a base station over a common channel through time-sharing[37]. The microfluidic TDMA resistive pulse sensor adopts a similar principle to multiplex the signal from many different fluidic channels. With a single-ended data acquisition, signals from each channel can be reconstructed for particle analysis in the corresponding channels. We successfully demonstrated an eight-channel microfluidic resistive pulse sensor for analyzing the size and concentration of polystyrene particles. Further scaling up the multiplexity is straightforward and within reach. We also found that the multiplexed TDMA device is able to continue the analysis even when a few channels are clogged, solving one of the most significant challenges in resistive pulse sensors. We anticipate this approach would facilitate developing multiplexed resistive pulse sensing from microscale to nanoscale.

II. EXPERIMENTAL

A. Microfluidic device fabrication

An eight-channel microfluidic device was designed using CAD software. The casting mold was fabricated on a 4-inch silicon wafer using SU-8 2025 (MicroChem) through a standard lithography process. The mold height of ~35 µm was confirmed with a profilometer. The width and length of the micropore were optimized to ~18 µm and ~20 µm respectively. A 10:1 w/w mixture of base and curing agent was cast onto the SU-8 wafer mold, degassed, and cured at 80°C for an hour. After demolding the patterned PDMS, inlet and outlets were punched using a stainless. The resulting PDMS stamps and glass slides were treated with oxygen plasma and in contact to form irreversibly covalent bonding between two materials.

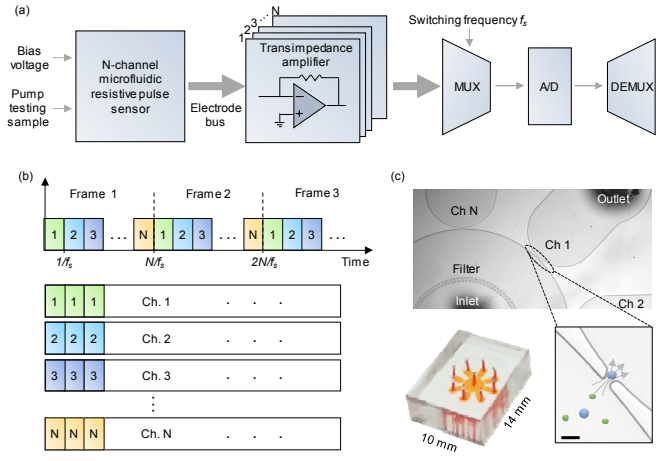

Fig. 1. TDMA resistive pulse sensor working principles. (a) Time-division multiple access block diagrams. (b) Illustration of the demultiplexing algorithm. The serial signal from multiplexer output was reconstructed for each channel. (c) Microscope images of the 8-plexed device.

978-1-7281-1634-1/19/$31.00 ©2019 IEEE

B. TDMA hardware instrumentation

The TDMA hardware circuit was implemented on a custom printed circuit board, which includes the trans-impedance amplifiers, analog multiplexer, and counter (Fig.1). Eight sensing units from the microfluidic device were connected to trans-impedance amplifiers, the output of which is connected as inputs to the multiplexer. The multiplexer channels were periodically selected by a $\log_2(N)$ bit synchronous counter. The sampling frequency for each TDMA frame was synchronized to the multiplexer switching frequency. The analog voltage output from multiplexer was sampled at 200 kHz with 16-bit DAQ card and stored through a data acquisition LabVIEW software. The recorded data were demultiplexed using MATLAB program.

C. Electrical measurement

The microfluidic channels were prefilled with electrolyte (1x PBS with 0.05% Tween-20) for electrical measurement. The Ag/AgCl electrodes were inserted in single inlet and eight outlets to apply a constant voltage (400 mV) across each sensing micropore. The ionic currents from each sensing unit were monitored by custom-built TDMA hardware. The electrical measurement was performed inside a customized Faraday cage to shield the environment noise. The sample was introduced at a constant flow rate using a syringe pump.

III. RESULTS AND DISCUSSION

A. Validation of the TDMA principle

To validate the 8-channel microfluidic resistive pulse sensor and the TDMA scheme, we tested polystyrene particles of 10 μm diameter at a concentration of ~2.4×10^5 particles/ml. Fig. 2 shows the demultiplexed current time traces for all eight channels. Apparent ionic current dips, corresponding to individual particle translocation events, could be easily observed from all channels. These current dips were uniform in magnitude due to the introduced monodisperse particles.

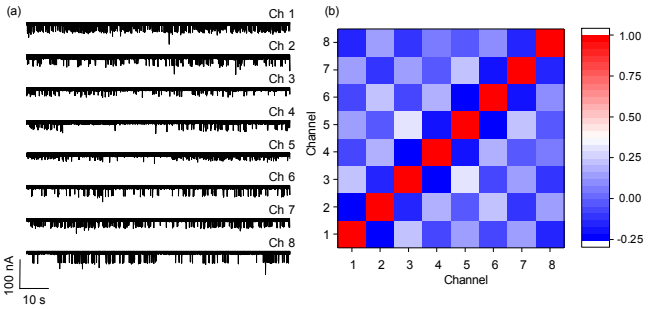

Fig. 2. Validation of TDMA resistive pulse sensor. (a) Reconstructed current time trace for each of the eight channels. (b) Cross-correlation among different sensing channels.

One of the concerns in TDMA resistive pulse sensing is the interference due to the signal leakage in analog switching networks. The current dips in Fig. 2a appear in random sequence, implying that each channel can independently analyze the particles without crosstalk among channels. To quantify the channel-to-channel crosstalk, we performed the cross-correlation analysis of ionic current profiles among eight sensing channels and extracted the Pearson correlation coefficient. Fig. 2b shows the heatmap of the correlation between channels. The inter-channel correlation is quite small (with coefficient ranging from -0.25 to 0.32), confirming the signal integrity in each channel.

B. Probing the particle arriving dynamics

A quick eyeball on the current time traces in Fig. 2a reveals that the particle translocation frequency varies among different channels. To probe the particle arriving dynamics, we examined the event inter-arrival time distribution for each channel. As shown in Fig. 3**,** the inter-arrival time distribution shows a remarkable exponential distribution for each channel, indicating a Poisson process[38]. Each channel was fitted with an exponential distribution $P(t)=\lambda e^{-\lambda t}$, where λ is the expected average time interval of the events. The average translocation rate can be derived by $1/\lambda$. As shown in Fig. 3**,** the particle inter-arrival time among different channels ranges from 0.32s to 1.27s, implying the introduced particles prefer certain channels. This is likely because the effective dimension for each sensing pore is not perfectly identical due to variations in the fabrication and the potential adsorption during the experiment. This creates asymmetric streamlines that lead the particles into preferred channels.

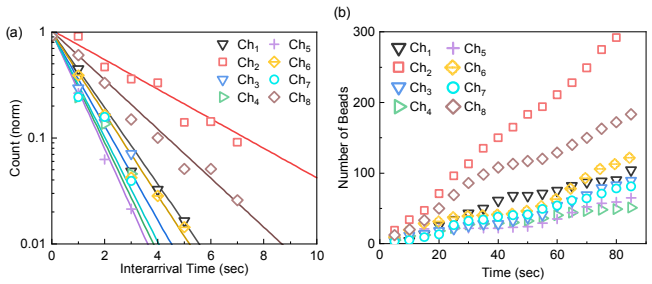

Fig. 3. Particle translocation dynamics. (a) The normalized distribution of bead interarrival time in different channels, with exponential fits to the distributions. (b) Cumulative counted particle numbers versus the elapsed time.

To further examine whether the observed Poisson process is homogenous or nonhomogeneous, we plotted the accumulative particle number versus the elapsed time. As shown in Fig. 3b**,** the slope of the curve (*i.e.,* the translocation rate) is different among channels, consistent with what we observed from Fig. 3b**.** However, the slope of the curve for each channel shows a clear time-dependence. This indicates the translocation rate for sub-processes indeed varies. Therefore, the particle translocation process of our experiment is a nonhomogeneous Poisson process.

C. Analyzing particle size and concentration

To test the multiplexed TDMA resistive pulse sensor for particle sizing, we extracted the relative resistance changes ($\Delta R/R$) from the detected resistive peaks in Fig. 2. To determine the particle size, we applied the particle sizing model [39]. Fig. 4a shows the particle diameter distribution in

each channel, together with a combined distribution from all channels. The combined distribution follows a Gaussian distribution with a mean value of ~9.5 ± 0.54 μm. The calculated particle diameter is comparable, yet smaller than the actual particle size (10 μm). The under-estimation of the particle diameter may come from the fact that the particle sizing model assumes particles pass through the centerline of the pore [39]. Motion displacement from the center axis could cause the underestimation. It was also observed that the mean particle diameter varies among eight individual channels (Fig.4a). This is likely due to the channel-to-channel size variation during the device fabrication and during the experiments (*e.g.*, adsorption of small debris near the pore region).

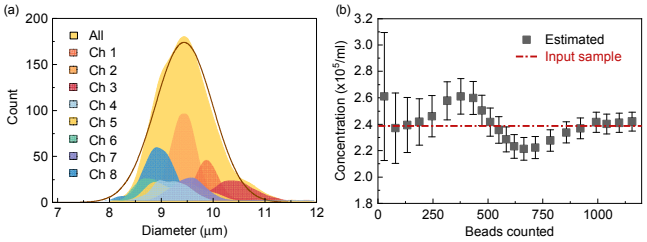

Fig. 4. Particle size and concentration measurement. (a) Histograms of the calculated particle diameters from each channel. (b) Calculated concentration as a function of the counted particles. The error bars correspond to the Poisson noise. The actual polystyrene particle concentration is indicated by the red dashed line.

Since each current dip event represents a single particle and the particle arriving events follow the Poisson process (Fig. 3), the particle concentration at 95% confidence interval was calculated as $(n \pm 1.96(n)^{1/2})/(vT)$, where n is the total number of particles counted from all 8 channels, T is the total elapsed time, and v is the volume flow rate. The relative uncertainty of inferring the concentration is proportional to $n^{-1/2}$. Fig.4b shows the calculated concentration as a function of total counted particles. After counting about 1000 particles, the calculated concentration converges to the input.

D. Analyzing a mixed population

To test the microfluidic multiplexed TDMA resistive pulse sensor for analyzing a mixed population, we prepared a mixed sample containing 10 μm and 15 μm polystyrene particles with concentrations of ~2.4×10^5 ml^{-1} and ~0.8×10^5 ml^{-1}, respectively. Fig. 5a shows the demultiplexed current time traces for all eight channels, and Fig. 5b shows an enlarged section from channel 4 (red boxed area). As expected, we observed two distinct levels of current dips, corresponding to the two size populations. Other channels also show similar two population characteristics. Using the particle sizing model [39] and combing events from all channels, the particle sizes were calculated, and their distribution is shown in Fig. 5c. The particle size distribution shows evident two populations with a mean value of 9.31 ± 0.40 μm (10 μm particle population) and 12.46 ± 0.48 μm (15 μm particle population), respectively. The underestimation for each population is likely due to the same reason as we saw in Fig. 4a**.** The particle numbers counted for each population is 1233 and 355, the ratio of which (~3.47) is close to that of the input concentration value (~3), confirming the discriminative ability between these two populations.

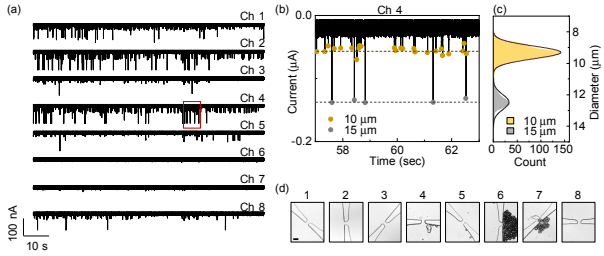

Fig. 5. Discriminating particles of different size. (a) Reconstructed current time trace for each of the eight channels. (b) Enlarged view of ionic current in channel 4. (c) Distribution of the particle size, with Gaussian-fit. A clear two population was observed. (d) Microscope images showing the pore clogging in channel 6 and 7. (Scale bar: 20 μm).

E. Robustness against pore clogging

While we did not see any clogging issue when testing the 10 μm sized particles (Fig. 2a), a clear feature observed in Fig. 5a when testing the 15 μm sized particles is that two out of eight channels (ch6 and ch7) show no particle translocation events. We examined the sensing pores using a microscope after the experiment. It was found that channel 6 and 7 were indeed clogged by particle jamming at the pore (Fig. 5d). This is not surprising since the pore cross-section is of dimension 18 μm×20 μm×35 μm (W×L×H). When 15 μm sized particles were introduced, the chance for clogging becomes much higher. Such irreversible clogging is a well-known issue for single-channel resistive pulse sensors that limits its flexibility in real-world applications[31, 32]. In contrast, the TDMA multichannel resistive pulse sensor allows the analysis to continue even when some of the pores are clogged (Fig. 5c). We anticipate that future works could introduce an array of different pore sizes for analyzing polydisperse samples.

IV. CONCLUSION

By introducing the time-division multiple access technique in the telecommunication field into the microfluidic field, we developed and demonstrated the multiplexed microfluidic resistive pulse sensor, in which particles can be analyzed simultaneously by a scalable number of microfluidic channels. In particular, the availability of multiple sensing pores provides a robust mechanism to fight against the clogging issue, allowing the analysis to continue, which is otherwise not possible in single channel devices. We expect this could be well extended to nanoscale resistive pulse sensors such as nanopores [40].

ACKNOWLEDGMENTS

This project was supported by a grant from the National Science Foundation, USA (ECCS-1710831). Support from Penn State Startup Fund was also acknowledged.

REFERENCE

1 Song, Y., Zhang, J., and Li, D.: 'Microfluidic and Nanofluidic Resistive Pulse Sensing: A Review', Micromachines, 2017, 8, (7), pp. 204

2 Gawad, S., Schild, L., and Renaud, P.H.: 'Micromachined impedance spectroscopy flow cytometer for cell analysis and particle sizing', Lab Chip, 2001, 1, (1), pp. 76-82

3 Watkins, N., Venkatesan, B.M., Toner, M., Rodriguez, W., and Bashir, R.: 'A robust electrical microcytometer with 3-dimensional hydrofocusing', Lab Chip, 2009, 9, (22), pp. 3177-3184

4 Nasir, M., Ateya, D.A., Burk, D., Golden, J.P., and Ligler, F.S.: 'Hydrodynamic focusing of conducting fluids for conductivity-based biosensors', Biosensors & bioelectronics, 2010, 25, (6), pp. 1363-1369

5 Dhawan, A.P., Heetderks, W.J., Pavel, M., Acharya, S., Akay, M., Mairal, A., Wheeler, B., Dacso, C.C., Sunder, T., Lovell, N., Gerber, M., Shah, M., Senthilvel, S.G., Wang, M.D., and Bhargava, B.: 'Current and Future Challenges in Point-of-Care Technologies: A Paradigm-Shift in Affordable Global Healthcare With Personalized and Preventive Medicine', IEEE J. Transl, Eng. He., 2015, 3, pp. 1-10

6 Emaminejad, S., Paik, K.H., Tabard-Cossa, V., and Javanmard, M.: 'Portable cytometry using microscale electronic sensing', Sens. Actuators, B, 2016, 224, pp. 275-281

7 Spencer, D., Caselli, F., Bisegna, P., and Morgan, H.: 'High accuracy particle analysis using sheathless microfluidic impedance cytometry', Lab Chip, 2016, 16, (13), pp. 2467-2473

8 Garboczi, E.J.: 'The influence of particle shape on the results of the electrical sensing zone method as explained by the particle intrinsic conductivity', Powder Technol, 2017, 322, pp. 32-40

9 Zheng Zhang, J.Z., Santanu Chandra, Jun Hu: 'An electronic pollen detection method using Coulter counting principle', Atmospheric Environment, 2005, 39, (30), pp. 5446-5453

10 Holmes, D., Pettigrew, D., Reccius, C.H., Gwyer, J.D., van Berkel, C., Holloway, J., Davies, D.E., and Morgan, H.: 'Leukocyte analysis and differentiation using high speed microfluidic single cell impedance cytometry', Lab Chip, 2009, 9, (20), pp. 2881-2889

11 Hua, S.Z., and Pennell, T.: 'A microfluidic chip for real-time studies of the volume of single cells', Lab Chip, 2009, 9, (2), pp. 251-256

12 Bernabini, C., Holmes, D., and Morgan, H.: 'Micro-impedance cytometry for detection and analysis of micron-sized particles and bacteria', Lab Chip, 2011, 11, (3), pp. 407-412

13 van Berkel, C., Gwyer, J.D., Deane, S., Green, N.G., Holloway, J., Hollis, V., and Morgan, H.: 'Integrated systems for rapid point of care (PoC) blood cell analysis', Lab Chip, 2011, 11, (7), pp. 1249-1255

14 Evander, M., Ricco, A.J., Morser, J., Kovacs, G.T.A., Leung, L.L.K., and Giovangrandi, L.: 'Microfluidic impedance cytometer for platelet analysis', Lab Chip, 2013, 13, (4), pp. 722-729

15 Zheng, Y., Nguyen, J., Wei, Y., and Sun, Y.: 'Recent advances in microfluidic techniques for single-cell biophysical characterization', Lab Chip, 2013, 13, (13), pp. 2464-2483

16 Rodriguez-Trujillo, R., Ajine, M.A., Orzan, A., Mar, M.D., Larsen, F., Clausen, C.H., and Svendsen, W.E.: 'Label-free protein detection using a microfluidic Coulter-counter device', Sens. Actuators, B, 2014, 190, pp. 922-927

17 Murphy, T.W., Zhang, Q., Naler, L.B., Ma, S., and Lu, C.: 'Recent advances in the use of microfluidic technologies for single cell analysis', The Analyst, 2018, 143, (1), pp. 60-80

18 Watkins, N.N., Hassan, U., Damhorst, G., Ni, H.K., Vaid, A., Rodriguez, W., and Bashir, R.: 'Microfluidic CD4(+) and CD8(+) T Lymphocyte Counters for Point-of-Care HIV Diagnostics Using Whole Blood', Sci Transl Med, 2013, 5, (214), pp. 214ra170(211-211)

19 van Berkel, C., Gwyer, J.D., Deane, S., Green, N.G., Holloway, J., Hollis, V., and Morgan, H.: 'Integrated systems for rapid point of care (PoC) blood cell analysis', Lab Chip, 2011, 11, (7), pp. 1249-1255

20 Yang, X.N., Chen, Z.F., Miao, J., Cui, L.W., and Guan, W.H.: 'High-throughput and label-free parasitemia quantification and stage differentiation for malaria-infected red blood cells', Biosensors & bioelectronics, 2017, 98, pp. 408-414

21 Yu, A.C.S., Loo, J.F.C., Yu, S., Kong, S.K., and Chan, T.F.: 'Monitoring bacterial growth using tunable resistive pulse sensing with a pore-based technique', Appl. Microbiol. Biotechnol., 2014, 98, (2), pp. 855-862

22 Song, Y.X., Zhang, H.P., Chon, C.H., Chen, S., Pan, X.X., and Li, D.Q.: 'Counting bacteria on a microfluidic chip', Anal. Chim. Acta, 2010, 681, (1-2), pp. 82-86

23 Yang, L., and Yamamoto, T.: 'Quantification of Virus Particles Using Nanopore-Based Resistive-Pulse Sensing Techniques', Frontiers in microbiology, 2016, 7, pp. 1500

24 Saleh, O.A., and Sohn, L.L.: 'Quantitative sensing of nanoscale colloids using a microchip Coulter counter', Rev. Sci. Instrum., 2001, 72, (12), pp. 4449-4451

25 Zhang, W.C., Hu, Y., Choi, G., Liang, S.F., Liu, M., and Guan, W.H.: 'Microfluidic multiple cross-correlated Coulter counter for improved particle size analysis', Sensors and Actuators B: Chemical, 2019, 296, (126615)

26 Waduge, P.a.H., R. and Bandrakar, P and Yamazaki, H and Cressiot, B and Zhao, Q. and Whitford, P and Wanunu, M: 'Nanopore-Based Measurements of Protein Size, Fluctuations, and Conformational Changes', Acs Nano, 2017, 11, (5), pp. 5706-5716

27 Hoogerheide, D.P., Gurnev, P.A., Rostovtseva, T.K., and Bezrukov, S.M.: 'Real-Time Nanopore-Based Recognition of Protein Translocation Success', Biophysical Journal, 2018, 114, (4), pp. 772-776

28 Karolis, M., E. Niklas , and U. F. Keyser: 'QuipuNet: Convolutional Neural Network for Single-Molecule Nanopore Sensing.', Nano letters, 2018, 6, pp. 4040-4045

29 Kidan, L., Kyeong-Beom, P., Hyung-Jun, K., Jae-Seok, Y., Hongsik, C., Hyun-Mi, K., and Ki-Bum, K.: 'Recent Progress in Solid-State Nanopores', Advanced materials, 2018, 30, pp. 1704680(1704681-1704628)

30 Rivas, F., Zahid, O.K., Reesink, H.L., Peal, B.T., Nixon, A.J., DeAngelis, P.L., Skardal, A., Rahbar, E., and Hall, A.R.: 'Label-free analysis of physiological hyaluronan size distribution with a solid-state nanopore sensor', Nat. Commun., 2018, 9, (1), pp. 1037

31 Maas, S.L.N., de Vrij, J., van der Vlist, E.J., Geragousian, B., van Bloois, L., Mastrobattista, E., Schiffelers, R.M., Wauben, M.H.M., Broekman, M.L.D., and Nolte-'t Hoen, E.N.M.: 'Possibilities and limitations of current technologies for quantification of biological extracellular vesicles and synthetic mimics', J. Control. Release, 2015, 200, pp. 87-96

32 Smeets, R.M.M., Keyser, U.F., Dekker, N.H., and Dekker, C.: 'Noise in solid-state nanopores', Proceedings of the National Academy of Sciences of the United States of America, 2008, 105, (2), pp. 417-421

33 Zhe, J., Jagtiani, A., Dutta, P., Hu, J., and Carletta, J.: 'A micromachined high throughput Coulter counter for bioparticle detection and counting', J Micromech Microeng, 2007, 17, (2), pp. 304-313

34 Osaki, T., Suzuki, H., Le Pioufle, B., and Takeuchi, S.: 'Multichannel simultaneous measurements of single-molecule translocation in alpha-hemolysin nanopore array', Anal Chem, 2009, 81, (24), pp. 9866-9870

35 Baaken, G., Ankri, N., Schuler, A.K., Ruhe, J., and Behrends, J.C.: 'Nanopore-based single-molecule mass spectrometry on a lipid membrane microarray', ACS Nano, 2011, 5, (10), pp. 8080-8088

36 Bell, N.A., Thacker, V.V., Hernández-Ainsa, S., Fuentes-Perez, M.E., Moreno-Herrero, F., Liedl, T., and Keyser, U.F.: 'Multiplexed ionic current sensing with glass nanopores', Lab Chip, 2013, 13, (10), pp. 1859-1862

37 Ozarow, L.H., Shamai, S., and Wyner, A.D.: 'Information-Theoretic Considerations for Cellular Mobile Radio', IEEE T. Veh. Technol., 1994, 43, (2), pp. 359-378

38 Meller, A., and Branton, D.: 'Single molecule measurements of DNA transport through a nanopore', Electrophoresis, 2002, 23, (16), pp. 2583-2591

39 Gregg, E.C., and Steidley, K.D.: 'Electrical Counting and Sizing of Mammalian Cells in Suspension', Biophys. J., 1965, 5, (4), pp. 393-405

40 Albrecht, T.: 'Single-Molecule Analysis with Solid-State Nanopores', Annual Review of Analytical Chemistry, 2019, 12, pp. 5.1–5.17